Acquiring and Using Realistic Reflectance Data in Computer Graphics Images

Joel DeYoung, Paul Lalonde, and Alain Fournier
University of British Columbia
Department of Computer Science
201-2366 Main Mall
Vancouver, BC, Canada
V6T 1Z4
{deyoung,lalonde,fournier}@cs.ubc.ca

Abstract

Analytical models of light reflection are in common use in computer graphics. However, as the sophistication of rendering methods has increased, analytical models have become less adequate for generating images. Reflectance data obtained by empirically measuring real world surfaces is needed to create more realistic looking images.

In this paper we examine several issues relevant to using measured reflectance functions in generating computer graphics images. We give an overview of the techniques involved in measuring and tabulating reflectance data. We compare and contrast measured reflectance functions with analytical illumination models, and evaluate several methods for interpolating tabulated reflectance functions. We also highlight potential areas of future research.

1 Introduction

The most fundamental operation in rendering computer graphics images is the computation of how light reflects off surfaces. This computation is often performed using a *local illumination model*. This is in contrast with a *global illumination model*, which is concerned with the interreflection of light between surfaces. Early models of local illumination emerged in the late 1960s. These early models, such as that due to Phong [12], were not based on physical principles of light reflection.

1.1 Analytical Models

More accurate local illumination models have been proposed by Blinn [2], Cook and Torrance [4] and He et al [10], using results from physics in the areas of radiative heat transfer and reflection from roughened surfaces. These are *analytical* models in that the reflection is computed from a closed form equation. The reflective properties of a given surface are manipulated with a relatively small number of parameters.

Many analytical models are restricted to representing simple isotropic surfaces. Isotropic reflection refers to reflection that does not vary as the surface is rotated about the vector perpendicular to the surface. Many surfaces in the real world exhibit much more complex behavior. Consequently, numerous extensions to analytical models have been proposed that allow the simulation of certain phenomena, including anisotropic reflection [13, 14], subsurface scattering [9], and wavelength dependence [8].

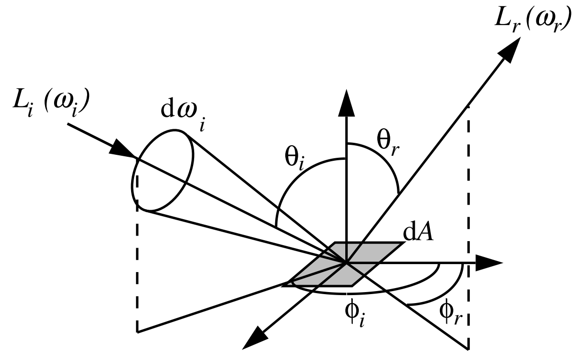

Figure 1: Shading Geometry

1.2 Bidirectional Reflectance Distribution Functions

Consider the geometry in Figure 1. Light arriving at a differential surface area dA through a solid angle

$d\omega_i$ from direction $\vec{\omega_i}$ is reflected in some other direction $\vec{\omega_r}$. The amount of reflected radiance L_r is proportional to the incident irradiance E:

$$dL_r(\vec{\omega_r}) \propto dE(\vec{\omega_i}), \quad (1)$$

The incident irradiance $E(\vec{\omega_i})$ can be rewritten in terms of the radiance from $\vec{\omega_i}$ and the solid angle $d\omega_i$:

$$E(\vec{\omega_i}) = L_i(\vec{\omega_i}) \cos\theta_i d\omega_i \quad (2)$$

The constant of proportionality in Equation 1 is called the bidirectional reflectance distribution function, or BRDF. Using the substitution from Equation 2, we can express the BRDF f_r as:

$$f_r(\vec{\omega_i} \to \vec{\omega_r}) = \frac{L_r(\vec{\omega_r})}{L_i(\vec{\omega_i}) \cos\theta_i d\omega_i} \quad (3)$$

The BRDF is a function in four variables (a polar and azimuth angle for each of the incident and reflected directions). It is often written as $f_r(\theta_i, \phi_i, \theta_r, \phi_r)$ to express this dependency explicitly. Note that in this form, f_r almost fully characterizes the anisotropic reflection of a surface, with several simplifying assumptions.

The first simplification we have made in Equation 3 is expressing the BRDF as independent of wavelength. This is physically incorrect, and means that we cannot express reflection from surfaces that cause the light to shift in frequency, such as thin film interference effects and reflection from metals. Furthermore, our definition of the BRDF ignores phenomena caused by subsurface scattering, as well as changes in the phase and polarization of the light.

For a more thorough treatment of the radiometric principles and terminology behind work in computer graphics illumination, the reader is referred to Glassner's book on digital image synthesis [7].

If we integrate over the hemisphere Ω_N surrounding dA, we get the fundamental reflectance equation:

$$L_r(\vec{\omega_r}) = \int_{\Omega_N} L_i(\vec{\omega_i}) f_r(\vec{\omega_i} \to \vec{\omega_r}) \cos\theta_i d\omega_i \quad (4)$$

Most work in computer graphics illumination has dealt with simplifying one or both of the L_i or f_r terms. In this paper, we are concerned with obtaining a BRDF (f_r) that accurately characterizes the reflectance behavior of real world surfaces.

2 Acquiring BRDF Data

In order to have realistic reflectance data, it would be ideal to take empirical measurements from actual surfaces. A device for taking such measurements is known as a *gonioreflectometer* (Figure 2). It works by moving a light source and detector over the hemispheres of incident and reflected directions, taking measurements every few degrees. These machines are relatively expensive and slow, and the data returned from them is often quite noisy.

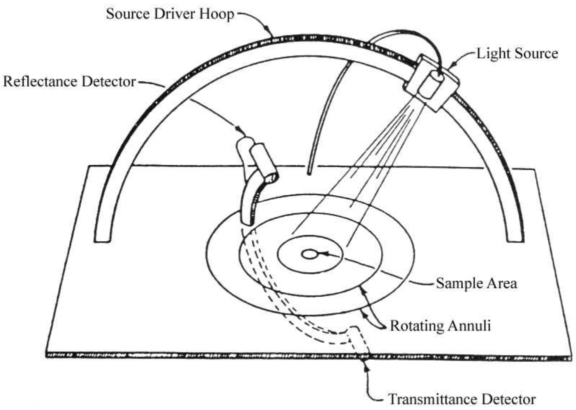

Figure 2: A simplified illustration of a gonioreflectometer.

Ward attempted to address the problems of cost and speed by building a novel implementation of a gonioreflectometer [14]. However, the samples obtained from his device are nonuniform, which complicates their use in rendering. Ward overcame this limitation by fitting the parameters of an anisotropic model to his data. This makes the data usable for rendering tasks, but his model limits the resulting images.

We have implemented a virtual gonioreflectometer in software. It uses a ray tracer to cast rays into a surface microgeometry. This approach is similar to previous attempts to measure BRDFs through simulation [3, 8, 15]. A small patch of the surface's microgeometry is modeled. For each combination of incident and reflected light directions, several positions on the patch are sampled stochastically, and the average of those samples is used as the value of the BRDF. Since all of the values are placed in a table, we refer to them as *tabulated* BRDFs (TBRDFs). Overall, this technique results in a BRDF that is representative of how light interacts with the surface when viewed from far enough away that the details of the microgeometry are not visible.

Figure 3 demonstrates this technique. On the left is a sawtooth microgeometry with alternating red and blue sides. On the right is a plane rendered with the resulting BRDF. Figure 4 shows two plots of the sawtooth BRDF. The black line shows the direction of incident light, while the colored blobs represent the distribution of reflected light. Visualizing the BRDF in this fashion, where the incident light direction can be manipulated interactively, is very useful when verifying that a TBRDF possesses certain reflective properties.

A more realistic example is shown in Figure 5. The red velvet microgeometry on the left was sampled with the virtual gonioreflectometer, and the resulting BRDF was used to render the cloth surface on the right.

3 Using Tabulated BRDFs

The most fundamental obstacle to using tabulated BRDFs is their large size. A TBRDF sampled at five degrees angular resolution, which is arguably sparse enough to miss highlights and other high frequency effects, can easily require over five million samples.

When devising a compression scheme for TBRDFs, it is fortunate to note that BRDFs are smooth over much of their range. However, they do contain discontinuities that are sufficiently important not to be ignored. Choosing an appropriate set of basis functions with which to represent the TBRDF should lead to considerable space savings.

3.1 Interpolation

When using TBRDFs in rendering, we need to be able to evaluate the BRDF at any position. For this reason, we must have a reliable way of interpolating between the samples.

The most naive method of interpolation is to use a piecewise constant strategy, simply choosing the closest sample point. While this technique is easy to implement, it is inadequate for even the simplest TBRDFs. The lack of continuity leads to highly visible artifacts (see Figure 6). Quadrilinear interpolation on the parameters $\phi_i, \theta_i, \phi_r, \theta_r$ provides geometric continuity, but the lack of tangential continuity leads to visible artifacts in some TBRDFs.

Higher order interpolation functions should provide us with more accurate reconstructions. In particular, we used a few different quadricubic interpolation methods. The simplest was to fit an interpolating tensor product cubic polynomial through the sixteen samples surrounding the requested sample point. We tried two versions of such an interpolating polynomial: one that maintained tangential continuity and one that did not. To achieve tangential continuity, we found a polynomial that fit a cubic $p(x)$ through sample points v_0, v_1, v_2, v_3 so that $p(0) = v_1, p(1) = v_2, p'(0) = v_2 - v_0$, and $p'(1) = v_3 - v_1$.

We also devised a quadricubic B-Spline scheme where we used the sample points as the B-spline control mesh. Note that in this case, the reconstructed BRDF does not pass through the sample points. However, it still produces good results because of the dense sampling over the hemisphere relative to the curvature of the BRDF. The TBRDFs in Figures 3 and 5 were interpolated using the B-spline scheme.

3.2 Results

Figure 7 shows the root mean squared error rates of several TBRDFs generated with a large number of samples and then re-sampled at a lower resolution.

The quadrilinear interpolation performed consistently well except for several visual artifacts caused by a lack of tangential continuity. This method was also the fastest, requiring only sixteen samples compared with the 256 required for the tensor product cubic methods. The interpolating splines proved to be a poor choice, due to the fact that interpolating splines often oscillate undesirably.

The best performer overall was the the B-Spline interpolation. Despite the fact that this method does not return exact values at the sample points, it provides a smooth tangentially continuous approximation of the BRDF. In terms of RMS error, it only performed worse than the other interpolation methods as the number of samples got very large.

4 Conclusion and Future Research

We have provided an overview of several issues involved in using tabulated reflectance functions. We have presented and compared several techniques for representing and interpolating TBRDFs. Based on the assumption that the TBRDF is acquired through uniform sampling, we found that B-spline interpolation provided the best reconstruction with the fewest samples.

Investigation into alternate representations of tabulated reflectance functions is needed. All of the techniques we have presented rely on the TBRDF being uniformly sampled. This is perhaps not the best approach since most BRDFs have large smooth areas but small areas where the function changes rapidly. The experiments presented in this paper must be extended to include schemes such as spherical harmonics [3], Forsey's hierarchical B-splines [6] and wavelet based reconstructions [11]. Methods of non-uniform interpolation are needed, since most currently obtainable sources of measured BRDF data are non-uniformly sampled [14].

It would also be interesting to measure certain properties of TBRDFs, and to devise techniques for transforming TBRDFs to possess those properties. This has the potential for filtering any noise introduced when acquiring the TBRDF, as well as simplifying the BRDF representation. These are all possibilities we are currently examining [5].

5 Acknowledgments

We gratefully acknowledge the support of the Natural Sciences and Engineering Research Council and the University of British Columbia Faculty of Graduate Studies for financially supporting this work. We wish to thank David Breen for supplying the cloth model used in Figure 5. Thanks also go to members of the Imager Computer Graphics Laboratory for their useful feedback.

References

[1] American National Standards Institute. ANSI standard nomenclature and definitions for illuminating engineering. ANSI/IES RP-16-1986, Illuminating Engineering Society, 345 East 47th Street, New York, NY 10017, June 1986.

[2] James F. Blinn. Models of light reflection for computer synthesized pictures. *Computer Graphics (SIGGRAPH '77 Proceedings)*, (July 1977), 192–198.

[3] Brian Cabral, Nelson Max, and Rebecca Springmeyer. Bidirectional reflection functions from surface bump maps. *Computer Graphics (SIGGRAPH '87 Proceedings)*, (July 1987), 273–281.

[4] R. L. Cook and K. E. Torrance. A reflectance model for computer graphics. *ACM Transactions on Graphics 1*, 1, (January 1982), 7–24.

[5] Joel DeYoung and Alain Fournier. Properties of tabulated bidirectional reflectance distribution functions. *Submitted for review, 1996.*

[6] David R. Forsey and Richard H. Bartels. Hierarchical B-spline refinement. *Computer Graphics (SIGGRAPH '88 Proceedings)*, (August 1988), 205–212.

[7] Andrew S. Glassner. *Principles of Digital Image Synthesis.* Morgan Kaufmann, San Francisco, 1995.

[8] Jay S. Gondek, Gary W. Meyer, and Jonathan G. Newman. Wavelength dependent reflectance functions. *Proceedings of SIGGRAPH '94 (July 24–29, 1994)*, Computer Graphics Proceedings, Annual Conference Series, 213–220.

[9] Pat Hanrahan and Wolfgang Krueger. Reflection from layered surfaces due to subsurface scattering. *Computer Graphics (SIGGRAPH '93 Proceedings)*, (August 1993), 165–174.

[10] Xiao D. He, Kenneth E. Torrance, Francois X. Sillion, and Donald P. Greenberg. A comprehensive physical model for light reflection. *Computer Graphics (SIGGRAPH '91 Proceedings)*, (July 1991), 175–186.

[11] Paul Lalonde and Alain Fournier. Shading with wavelet compressed tabulated reflectance functions. *Submitted for review, 1996.*

[12] Bui-T. Phong. Illumination for computer generated pictures. *Communications of the ACM 18*, 6, (June 1975), 311–317.

[13] Pierre Poulin and Alain Fournier. A model for anisotropic reflection. *Computer Graphics (SIGGRAPH '90 Proceedings)*, (August 1990), 273–282.

[14] Gregory J. Ward. Measuring and modeling anisotropic reflection. *Computer Graphics (SIGGRAPH '92 Proceedings)*, (July 1992), 265–272.

[15] Stephen H. Westin, James R. Arvo, and Kenneth E. Torrance. Predicting reflectance functions from complex surfaces. *Computer Graphics (SIGGRAPH '92 Proceedings)*, (July 1992), 255–264.

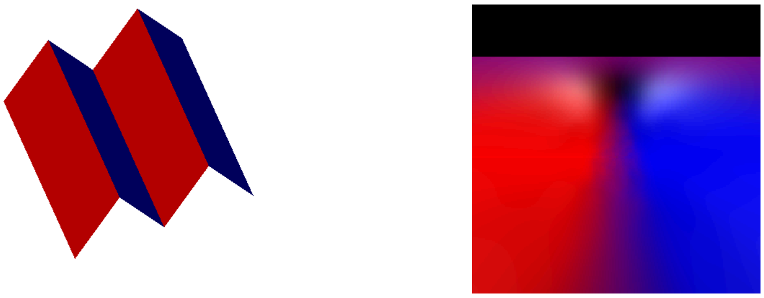

Figure 3: The sawtooth microgeometry (left) and sawtooth plane (right).

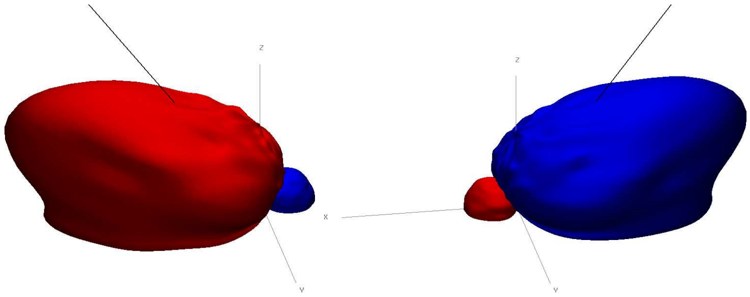

Figure 4: Two plots of the sawtooth BRDF. The direction of the incident light is designated by the black line. On the left, the light is coming from ($\theta_i = 30.0, \phi_i = 0.0$). On the right, it is coming from the other direction ($\theta_i = 30.0, \phi_i = 180.0$).

Figure 5: A red velvet microgeometry (left) and the resulting BRDF applied over a cloth surface (right).

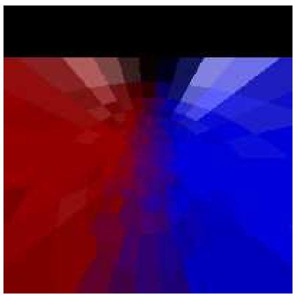

Figure 6: The sawtooth plane from Figure 3 rendered with piecewise constant interpolation.

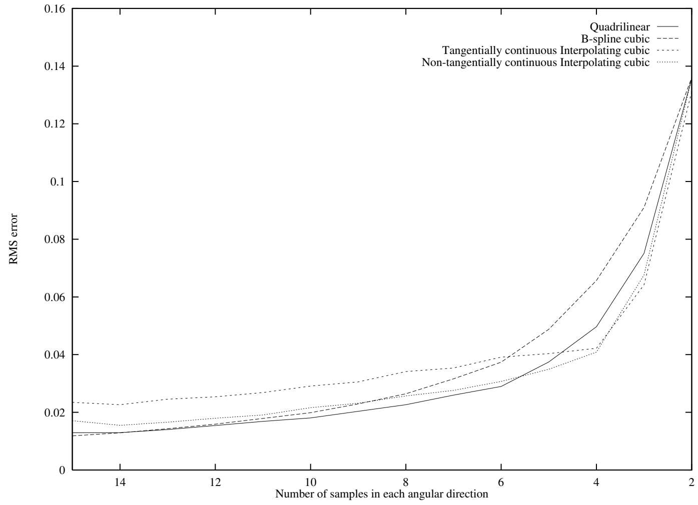

(a)

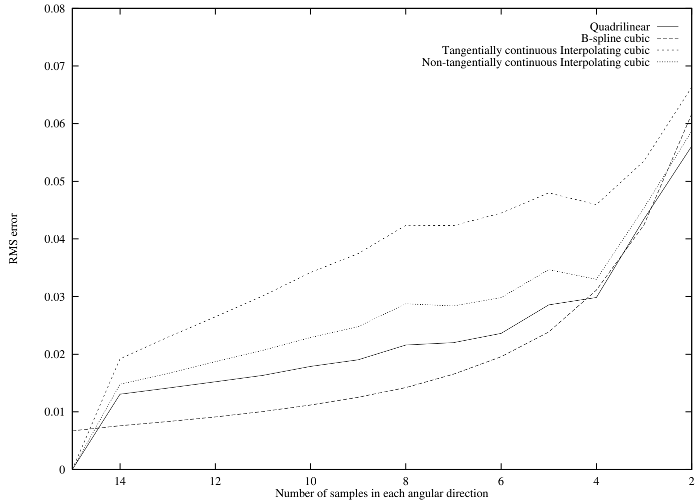

(b)

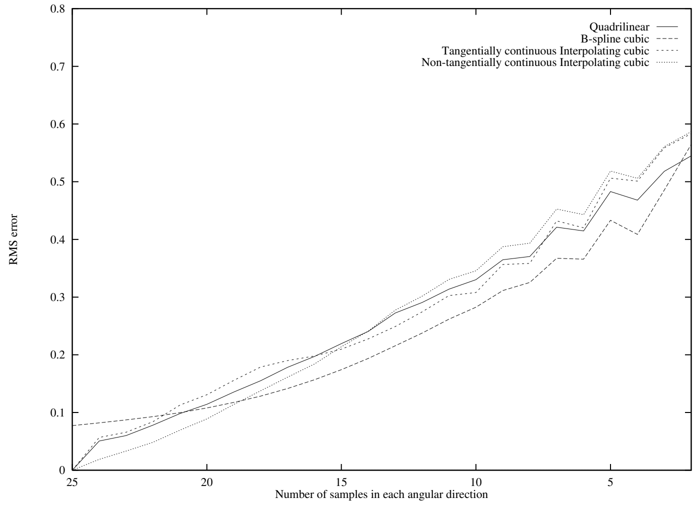

(c)

Figure 7: Root mean squared error for three TBRDFs: (a) TBRDF generated from a sawtooth microgeometry (Figure 3) originally sampled at a resolution of 30 samples in ϕ_i and ϕ_r and 15 samples in θ_i and θ_r; (b) TBRDF generated from a velvet microgeometry (Figure 5) originally sampled at a resolution of 15 samples in each angular direction; (c) TBRDF generated from the Phong analytical model, originally sampled at a resolution of 25 samples in each angular direction.